A Vision-based Inspection Strategy for Large-scale Photovoltaic Farms Using an Autonomous UAV

Zhipeng Xi[1], Zhuo Lou[1], Yan Sun[1], Xiaoxia Li[1], Qiang Yang[1,2], Wenjun Yan[1]
[1]College of Electrical Engineering, Zhejiang University, Hangzhou, 310027 China
[2]Jiangsu Key Construction Laboratory of IoT Application Technology, Taihu University of Wuxi, Wuxi, 214064
qyang@zju.edu.cn

***Abstract*— The complex operational environment of photovoltaic farms has brought direct challenges to the conventional manual-style inspection. Small-scale quad-rotor unmanned aerial vehicles (UAVs) have been widely used in many civil applications in virtue of their obvious advantages. A typical UAV based inspection system aims to obtain infrared and visible images of polar panels to detect the failures; usually, the process of acquiring the images relies on manual work or autonomous flight control according to previously obtained waypoints, and the disadvantages of the above methods are inefficiency and inaccuracy respectively. In this paper, a vision-based image acquisition strategy is presented without predefined task points. Firstly, single PV string's edges are acquired by processing video frames in real time; then the flight direction and offset for the UAV can be calculated; through the velocity control algorithm, automatic tracking for PV arrays can be achieved. The proposed solution is evaluated through experiments and the numerical results demonstrated the effectiveness of the suggested approach.**

Keywords-PV inspection; Quad-rotor UAV; vision-based control

I. INTRODUCTION

The National Energy Administration indicated that China added 53.06GW of PV installed capacity in 2017 and it has become the country with the biggest capacity of solar power across the world. With the development of low-carbon economy and technological advances, a various forms of renewable energy resources are playing an increasingly important role in energy provision.

Due to the rapid development of solar photovoltaic power generation, the efficient inspection for PV plants has been attached great significance during the whole operation period lasting for 20 to 25 years. A new challenge should be noticed that the inspection technology for PV panels in large farms is far from mature. The Autonomous unmanned aerial vehicles (UAV) based platforms commonly rely on Global Positioning System (GPS) and the position coordinate are mainly used to supply waypoints for UAVs to follow; nevertheless, the position information of PV panels can hardly be obtained accurately and errors in GPS measurement are widely existed. Meanwhile, manual operation apparently decreases the efficiency as well as violates the original intention of automation. Such conventional inspection methods cannot meet the demand of efficiency and accuracy, and even not feasible to be carried out in large-scale PV farms, e.g., with the capacity of tens of megawatts.

Under such circumstances, other control variables are required for local position feedback so that the expected flight path could be accomplished. Vision-based control strategy is a simple but practical scheme. A collection of research effort has been made in the literature. The work in [1] aimed to detect the overhead power lines and they effectively distinguished the power lines from the various illumination conditions. The visual control of UAVs was adopted in [2] to crop inspection in 2017 and the UAV is oriented in straight lines that are found in areas of structured crops. The study in [3] designed a vision-based line following system to guide an autonomous UAV to follow water channel margins in 2015. The authors have displayed experimental results of the proposed systems. Real-time algorithms for calculating on the basis of image processing have wide applications in many domains [4-7].

Figure 1. The illustration of PV inspection using an UAV

This work presents a vision-based inspection strategy for large-scale photovoltaic farms. The main technical contributions made in this work can be summarized as follows: (1) the whole process of UAV-based PV image data acquisition is clearly defined in details and (2) simple and reliable vision-based flight control is presented and achieved. To the best of our knowledge, this is the first study that jointly considers vision servo control and inspection in large-scale photovoltaic farms.

The rest of the paper is organized as follows: section II discusses obtaining mission areas and the pre-processing method; section III involves video frames processing and calculating; section IV analyzes speed control strategy upon the foundation of section III; and experimental results and conclusive remarks are given in section V.

II. MISSION AREAS ACQUISITION

A. Boundary acquisition

The boundary information can be gained from design drawings of the photovoltaic plant, GPS, and aerial images together with Geographic Information Systems (GIS). Precise position information of PV panels is unneeded, and only distribution feature and the boundary shape of the region are involved which is completely different from waypoints based flight strategy.

978-1-5386-7445-1/18/$31.00 ©2018 IEEE
DOI 10.1109/DCABES.2018.00059

The following operation effectively transforms the region boundary from irregular shape to polygons. For the sake of simplicity, the number of edges of each polygon to 4-8 is appropriate. Generally speaking, the circumscribed polygons of the area have certain subjectivity and randomness, but the difference would have no impact on the final results. As an example, Fig.2 demonstrates the way of generating circumscribed polygons.

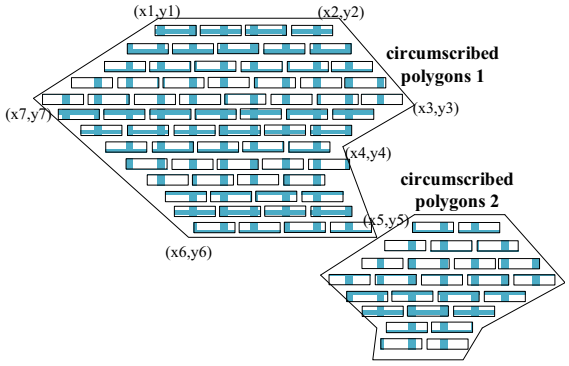

Figure 2. The way of generating circumscribed polygons

B. Subareas generation

The polygons created above may not meet the requirements and subsequent treatment is necessary. The rules can be listed as follows:

- R010: if two polygons are connected, they should be regard as a single polygon.
- R020: construct convex polygon for the concave polygons after applying R010; divide the difference area into several parts according to connectivity of the difference area.
- R030: if any difference area from R020 intersects with the convex polygon, has vast space span in the east-west direction and intersects with original concave polygons both in the east and west direction, the primary concave polygon need to be decomposed and cannot be considered as "Regional Polygon", which means the polygon can be used directly for UAVs to perform flight tasks in the paper.
- R040: all the convex polygons can be treated as "Regional Polygons".
- R050: the principle of decomposition in R030 is min-sum of spans in N-S direction and all polygons being "Regional Polygons" after decomposition.

After the above treatments, the various PV plant shapes can be decomposed into "Regional Polygons" as shown in Fig. 3. There is no detailed discuss due to limited space. In general, swarm intelligence algorithms can be employed to optimize the inspection sequence and start points of "Regional Polygons", which is not involved in the article.

C. Start Point Determination

Specific to each "Regional Polygon", start point can be select from the vertices located in northern or southern edges. For "Regional Polygon 1" in Fig. 3, when $S_1(x_1, y_1)$ is chosen, $\vec{v}_{1t}$ and $\vec{v}_{1n}$ are original flight direction and cruising direction, respectively.

III. Line Detection and Calculating

The reference for velocity control of UAV is calculated by the PV string edge detection and calculation algorithm, the process of which comprises of three steps. On the first step, images are converted from RGB to HSV color space and Canny edge detection is introduced. On the second step, Hough Transform is applied to detect straight lines. Finally, slope of the edge lines and offset from the image center are calculated. The main steps are described below respectively.

A. Edge Detection

In the large-scale farms, PV panels are easily distinguished from the background environment due to the obvious color features, which have better expression in HSV color space.

Video frame from the downward looking camera is the image data to be processed. Resizing and median filtering technologies are utilized in image pre-processing to reduce computation and the effect of noise. Predefined threshold can screen the pixels belonging to panels in HSV color space. Although light may affect the result, further procedure demonstrates the robustness for the case.

Because the objects we are dealing with are PV strings, morphological method is applied to make adjacent panels connected. Edge information can be extracted precisely through Canny edge detector.

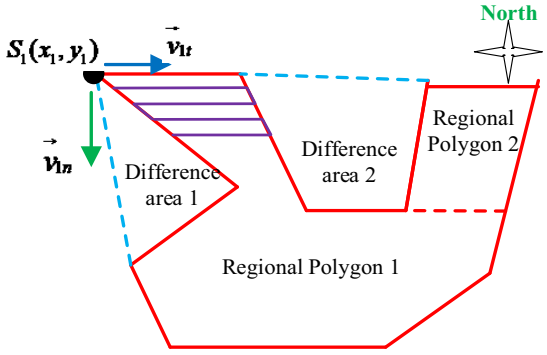

Figure 3. Diagram of original concave polygon, difference areas and regional polygons

B. Line Detection

Hough transform is adopted to identify straight lines in binary edge image. Previous steps have achieved the maximum resistance to external disturbances, and accurate acquisition of edge lines is achievable. The main disturbing lines come from vertical direction (determined by the direction of camera) of current PV string and other strings, and eliminating these line is necessary.

The length is the primary feature because only true edges can form long lines; too short lines may be caused by light. The slope is the most significant character and lines with big absolute value of slope cannot be top or bottom edges in the video frames. So the target lines should comply with the following requirements.

$$\begin{cases} len\_line > len\_threshold \\ |k\_line| < k\_threshold \end{cases} \quad (1)$$

where $len\_threshold$, $k\_threshold$ are the thresholds of length and slope, respectively.

C. Slope and Offset Calculation

Upper and lower edge lines screened out, average slope and pixel distance between image center and center line of current PV string can be calculated as follows:

$$k\_ave = (\sum_{i=1}^{p} k\_upper + \sum_{i=1}^{q} k\_lower) / (p+q) \quad (2)$$

$$pix\_err = (\sum_{i=1}^{p} dis\_upper) / 2p + (\sum_{i=1}^{q} dis\_lower) / 2q - img\_h \quad (3)$$

Where p, q are the number of upper and lower edge lines respectively, and img_h is the height of resized video frames. For the sake of lens distortion and various heights of the whole PV string, p and q instead of 1 are used. Fig.4(a) is video frame, Fig.4(b) shows segmentation result in HSV color space, Fig.4(c) exhibits the contour line and Fig.4(d) is the diagram of calculating pix_err.

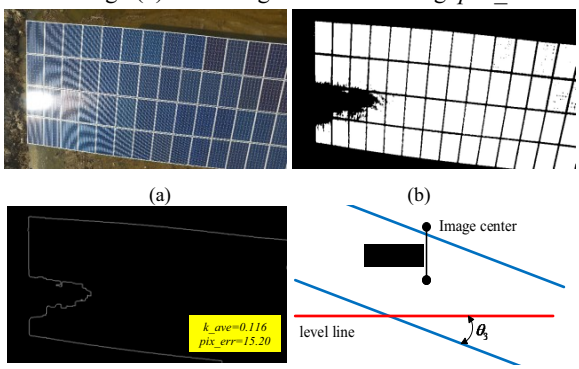

Figure 4. Diagram of contour line extraction and offset calculation

IV. Velocity Controller

According to the actual characteristics of PV power system, all the PV strings present an approximate east-west trend, which is the foundation of our approach. In order to simplify the analysis of fault locating and image processing, ideal target PV string in the images possesses the following characteristics: locating in the center of the pictures, and edges being parallel to the upper and lower borders. Aiming at this purpose, yaw angle of the gimbal and velocity of the drone should be taken into consideration. The flight process can be divided into tracking and turning.

A. Tracking Procedure

In NED (North East Down) coordinate, the relationship among yaw angle of the drone θ_1, yaw angle of the gimbal θ_2 and inclination angle of the PV string θ_3 can be described as Fig.5. θ_1 and θ_2 can be gained from onboard processor and θ_3 can be calculated as:

$$\theta_3 = \arctan(k\_ave) \quad (4)$$

Thus the direction of the PV string can be expressed as:

$$\theta = \theta_1 + \theta_2 + \theta_3 \quad (5)$$

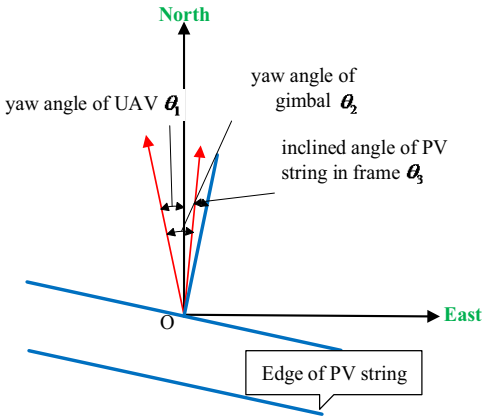

Figure 5. Relationship of drone yaw, gimbal yaw and PV string inclination angle

Usually, $\theta = 0$, which means the string has a east-west arrangement. Distance between PV string center and image center is:

$$d\_err = pix\_err / img\_h * H * \tan(0.5 * FOV) \quad (6)$$

where H is the flight height, and FOV means Field of View.

The control objective is minimize both gimbal yaw deviation and d_err and keep a constant speed along PV strings simultaneously. The adjustment of gimbal yaw is:

$$\Delta\theta_2 = \theta_3 \quad (7)$$

Meanwhile, speed control strategy can be expressed as:

$$\begin{cases} v_x = -v_0 \sin\theta + k * d\_err \\ v_y = v_0 \cos\theta \end{cases} \quad (8)$$

As illustrated in Fig.6, the velocity aims to realize efficient tracking control and eliminate deviation from image center. In consideration of the complexity and inherent deviation of UAV system and accuracy demand of images, simple calculation process and control form are quite ideal, which can explain why complicated control strategy is not involved. Still, necessary measures should be taken to avoid oversized d_err; accordingly, k can be set as follows:

$$k = \frac{b}{a + |d\_err|} \quad (9)$$

where a, b are positive constants. Formula (7) and (8) constitute the core of the control in the stage of tracking.

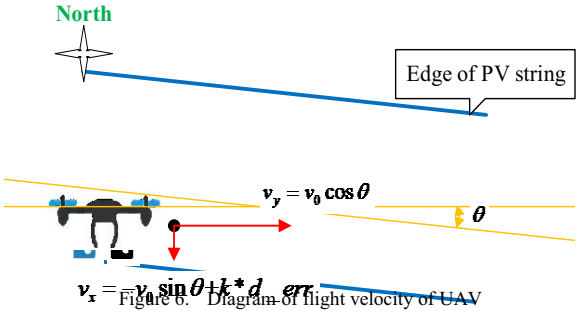

Figure 6. Diagram of flight velocity of UAV

B. *Turning procedure*

One of the most important roles of vertices generated in Part II is judging the real-time location of UAV in the region. Considering that possible errors may cause incomplete image data, formula (10) is presented to confirm the real location:

$$\frac{\sum_{i=1}^{pix\_n} x_i}{pix\_n} \geq ColorThreshold \tag{10}$$

where pix_n is the total number of pixels of the whole video frame, $x_i \in \{0,1\}$ is the pixel value in the binary image after converted to HSV color space in Part III and *ColorThreshold* represents the threshold to determine whether there is a PV string in the current video frame. A complete description of UAV crossing the boundary of "Regional Polygon" can be expressed as that current location point of UAV is not inside the "Regional Polygon" and formula (10) is not satisfied. Thus, if the UAV has arrived the border, the following steps should be performed.

As illustrated in Fig.7, the overall turning procedure of UAV during the PV farm inspection can be described as follows: (1) step #1: fly a distance that approximately equals to interval of two adjacent PV strings along the cruising direction; (2) step #2: fly in the same or reverse speed direction as that of previous string until the UAV has reached the boundary of "Regional Polygon"; and (3) step #3: continue the image acquisition task along the direction contrary to that in last string.

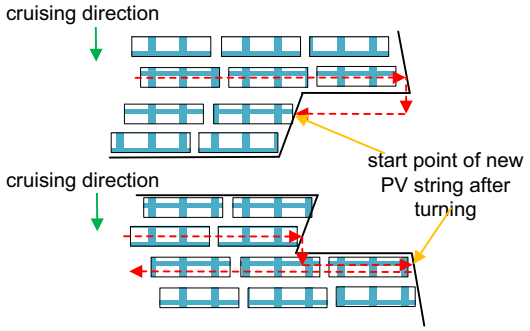

Figure 7. Schematic of turning procedure

V. Experimental Results and Conclusion

The quad-rotor used in the experiments was Matrice 100 of DJI, verified the algorithm's stability and accuracy. Fig.1 recorded one scene of the tests. Matrice 100 is equipped with a high-performance onboard processor which can achieve both video stream acquisition and image processing. Through the control instructions already encapsulated, stable and accurate flight can realize. Fig.8 demonstrates boundary lines extracted through Hough transformation and the screened ones, indicating accurate results of angle and distance calculation.

In summary, we have presented a vision-based image acquisition strategy for large-scale PV plants. PV inspection system by UAV has enormous advantages for its efficiency and automation. According to our research achievements in the field, visual servo control and automatic flight control are combined firstly, and the issue has been divided into mission areas acquisition, line detection and calculating, and velocity control. All the technical details are included in these three parts and well represented in a short space.

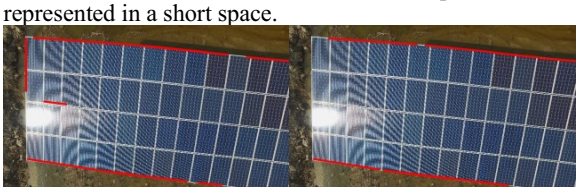

Figure 8. Boundary lines through Hough transform and screened ones

The limitations of the presented algorithm include the following aspects: first, recognition algorithm of PV panels under complex background should be considered, and combining color and texture features is a feasible method; second, above-mentioned steps and approaches is not applicable to distributed PV plants built mainly on the roofs; third, reasonable start point planning and task allocation for multiple UAVs could be of great significance due to limited power and communication distance. In the field of UAV-based PV inspection, pioneer researches remain to be explored.

Acknowledgement

This work is supported by the National Natural Science Foundation of China (51777183), the Natural Science Foundation of Zhejiang Province (LZ15E070001), and the Natural Science Foundation of Jiangsu Province (BK20161142).

References

[1] T. W. Yang et al., "Overhead power line detection from UAV video images," 2012 19th International Conference on Mechatronics and Machine Vision in Practice (M2VIP), Auckland, 2012, pp. 74-79.

[2] J. A. Sarapura, F. Roberti, R. Carelli and J. M. Sebastián, "Passivity based visual servoing of a UAV for tracking crop lines," 2017 XVII Workshop on Information Processing and Control (RPIC), Mar del Plata, 2017, pp. 1-6.

[3] A. S. Brandão, F. N. Martins and H. B. Soneguetti, "A vision-based line following strategy for an autonomous UAV," 2015 12th International Conference on Informatics in Control, Automation and Robotics (ICINCO), Colmar, 2015, pp. 314-319.

[4] C. Martinez, C. Sampedro, A. Chauhan and P. Campoy, "Towards autonomous detection and tracking of electric towers for aerial power line inspection," 2014 International Conference on Unmanned Aircraft Systems, Orlando, FL, 2014, pp. 284-295.

[5] C. L. Hwang and H. H. Huang, "Experimental validation of a car-like automated guided vehicle with trajectory tracking, obstacle avoidance, and target approach," IECON 2017 - 43rd Annual Conference of the IEEE Industrial Electronics Society, Beijing, 2017, pp. 2858-2863.

[6] Q. Li, Y. Tan, Z. Huayan, S. Ren, P. Dai and W. Li, "A visual inspection system for rail corrugation based on local frequency features," IEEE 14th Intl Conf on Dependable, Autonomic and Secure Computing, 14th Intl Conf on Pervasive Intelligence and Computing, 2nd Intl Conf on Big Data Intelligence and Computing and Cyber Science and Technology Congress, Auckland, 2016, pp. 18-23.

[7] H. Huang, H. Zhou, H. d. Qin and M. w. Sheng, "Underwater vehicle visual servo and target grasp control," 2016 IEEE International Conference on Robotics and Biomimetics (ROBIO), Qingdao, 2016, pp. 1619-1624.